Organization of Zeolite Microcrystals for Production of Functional Materials

KYUNG BYUNG YOON

Center for Microcrystal Assembly, Department of Chemistry, and Program of Integrated Biotechnology, Sogang University, Seoul 121-742, Korea

Received May 31, 2006

ABSTRACT

This Account summarizes various methods of organizing zeolite microcrystals into two-dimensional functional entities such as monolayers, multilayers, and patterned monolayers on various substrates and three-dimensional functional entities such as microballs and protein−zeolite composite fibrils. In the case of monolayer assembly, various types of linkages and substrates, factors that govern the rate, degree of coverage, degree of close packing, degree of uniform orientation, and average binding strength between each crystal and the substrate are described. The current and future applications of the organized products are also discussed.

Introduction

The ability to rationally assemble complex structures from modular components of various sizes is an essential part of life and key to success for the materials chemistry of the new millennium.[1] Chemists have acquired enough ability to organize subnanometer building blocks such as atoms and small molecules into complex structures. With the dawn of a new century, chemists have begun including nanobuilding blocks (1−10 nm) into their pools of building blocks. However, micrometer-sized building blocks have not yet been considered as a class of building blocks despite the fact that the ability to organize them will make materials chemistry flourish.

Using zeolite microcrystals as model microbuilding blocks, we developed methods of organizing them into two- (2D) and three-dimensionally (3D) organized structures.[2−22] The use of zeolite microcrystals as microbuilding blocks has additional merit since each zeolite microcrystal has millions of regularly spaced nanochannels and billions of nanopores which can be filled with a variety of functional molecules or nanoparticles. Therefore, we intended to not only develop the 'chemistry of microbuilding blocks' but also open a gateway to application of zeolites as advanced materials.

Kyung Byung Yoon received his B.S. degree in 1979 from the Department of Chemistry, Seoul National University. In 1981, he obtained his M.S. degree from the Department of Chemistry, Korea Advanced Institute of Science and Technology (KAIST), Seoul. From 1981 to 1984 he was employed by Chon Engineering Co. Ltd., Seoul, Korea. In 1989, he earned his Ph.D. degree in Inorganic Chemistry from the Department of Chemistry, University of Houston, Houston, Texas, where his research advisor was Professor Jay K. Kochi. He has been an Assistant, Associate (1993), and Professor (1998) in Sogang University, Seoul, Korea from 1989 to the present.

10.1021/ar000119c CCC: $37.00
Published on Web 10/04/2006

This Account summarizes the methods of organizing zeolite microcrystals and the imminent and future applications.

Modes of Reaction Promotion

We used three different modes of reaction promotion; reflux and stirring, sonication without stacking, and sonication with stacking (Figure 1).[2−6,20] In reflux and stirring, the functional-group-tethering glass plates are placed on a Teflon support and a stirring bar is rotated under the support while reflux proceeds. In sonication without stacking, the functional-group-tethering glass plates are placed individually on a comb-shaped support placed at the bottom of a flask. Sonication is carried out using an ultrasonic bath. In sonication with stacking, a functional-group-tethering glass plate is interposed between two bare glass plates and each stack of three glass plates is placed on the comb-shaped support.

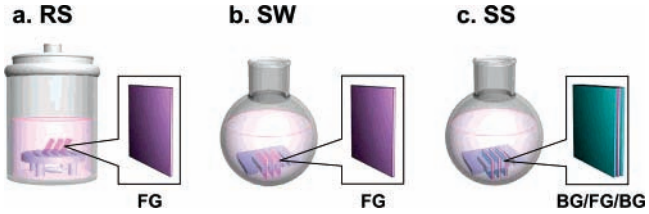

FIGURE 1. Illustration of reflux and stirring (RS), sonication without stacking (SW), and sonication with stacking (SS). The functional-group-tethering glass (FG) and bare glass (BG) plates are purple and green, respectively.[20]

Monolayer Assembly with Covalent Linkages

Mallouk, Bein, and Calzaferri attempted the attachment of zeolite microcrystals on substrates as a means to modify electrode surfaces[23−25] and grow continuous zeolite films.[26,27] However, the coverage, close packing, and uniform orientation were not satisfactory. We have shown that the above factors increase dramatically when the crystal sizes are uniform and the crystal faces are flat. Functional groups were tethered to the surfaces of zeolite and substrates by sylilation[2−4,6−13,17−22] and urethanation.[15]

Our first demonstration was the monolayer assembly of aminopropyl-tethering zeolite-A microcrystals on 3-(2,3-epoxypropoxy)propylsilyl (EP)-coated glass plates (18 × 18 mm^2) with reflux and stirring (Figure 2).[2] The scanning electron microscope (SEM) image (Figure 3a) shows that the microcrystals readily assemble into uniformly oriented monolayers on the entire glass plates with high degrees of coverage (>90%), close packing, and uniform orientation, indicating that amine−alcohol linkage formation readily takes place. ZSM-5 (Figure 3b) and various other crystals with a size larger than 2 μm also readily formed monolayers on glass with similar degrees of coverage, close packing, and uniform orientation.

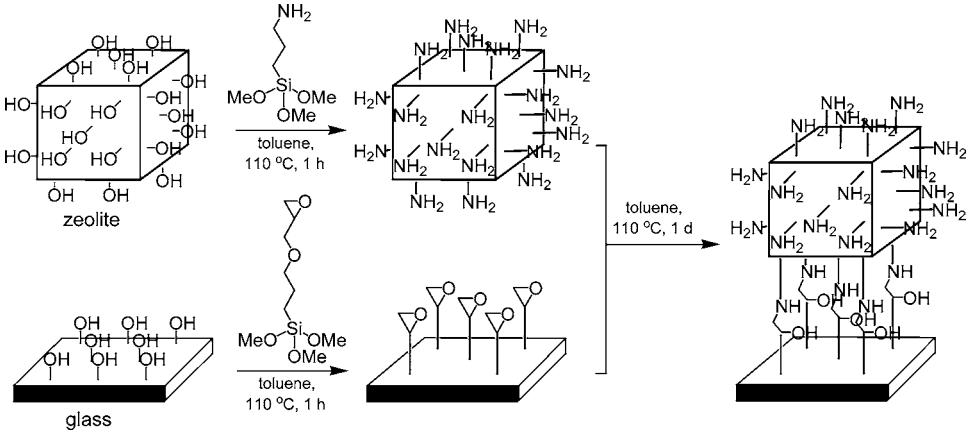

FIGURE 2. Procedure to attach zeolite-A crystals onto glass through surface-tethered aminopropyl and EP groups.[2]

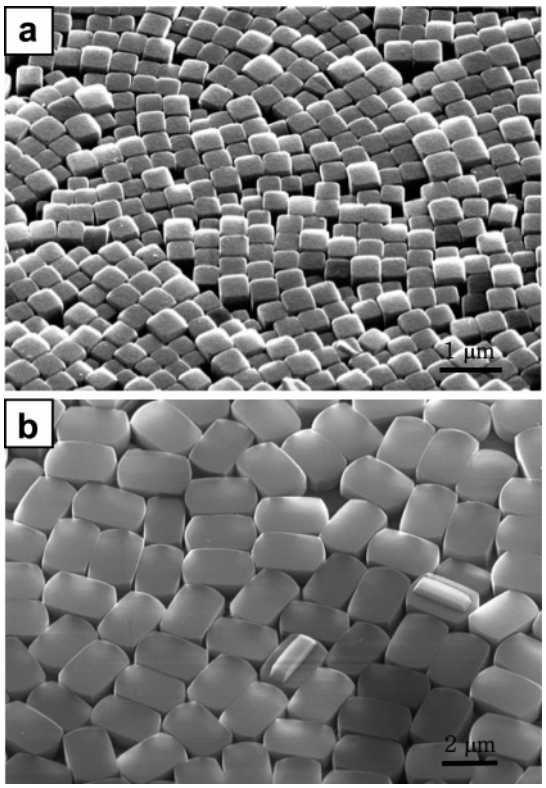

FIGURE 3. SEM images of zeolite A (a) and silicalite-1 (b) microcrystal monolayers assembled on glass.[2]

Attachment of a crystal with a size of $2 \times 2 \times 2\ \mu m^3$ onto a glass plate through 1-nm-long molecular linkers is analogous to attachment of a rock with a size of $60 \times 60 \times 60\ m^3$ onto a large wall using a large number (≤2.6 million) of strings with a length of 3 cm and thickness of 3 mm.[28] The size limit of the covalently attachable zeolite crystals was $\sim 10 \times 10 \times 10\ \mu m^3$.

Among various covalent linkages (Figure 4a−g)[3,4,6,8,15,19] the ether linkage formed by reaction between surface-tethered halopropyl groups and hydroxyl groups (Figure 4g)[4] has been most widely used due to its simplicity. Characterization of different types of linkages in terms of number density, thickness, and roughness of each linker was possible by X-ray reflectivity.[29]

Monolayer Assembly with Ionic Bonding.

Sodium-butyrate-tethering silicalite-1 crystals readily formed monolayers on trimethylpropylammonium-iodide-tethering glass plates (Figure 4h) in ethanol.[9] The binding strengths were substantially higher than those of the zeolite crystals covalently attached onto glass, indicating that the amount of linkage between each zeolite crystal and glass is higher with ionic than with covalent linkage due to the following. Ionic bonding is omnidirectional, works well regardless of the distance between the positive and negative centers, and does not require kinetic energies for bond formation. Mono- or multilayers of polyelectrolytes can also be used as the intermediate layers (Figure 4i). Use of aminopropyl/negative polyelectrolyte/aminopropyl linkage even in an acidic medium leads to formation of monolayers with poor coverage and close packing.[27]

Monolayer Assembly with Hydrogen Bonding

Thymine-tethering silicalite-1 crystals (2.5 μm) readily formed closely packed monolayers on adenine-tethering glass plates in an aqueous solution at room temperature (Figure 4j).[12] At the annealing temperature (55 °C), at which bond breaking and bond reforming between the surface-tethered complementary DNA bases become very rapid, the assembly rate and degree of close packing increased significantly due to faster surface migration of the crystals.

Monolayer Assembly with Physical Adsorption

Calzaferri,[30] Tsapatsis,[27,31] and Ban and Takahashi[32] demonstrated that zeolite microcrystals can also be organized in the form of closely packed monolayers on substrates by physical adsorption of the microparticles onto substrates. The adsorption methods were slow evaporation,[30] dip coating,[27,32] and convective assembly (vertical deposition).[31] Polystyrene can also be applied for stronger adhesion.[26] Yan and co-workers[33] elucidated that in-situ monolayer assembly of the nanocrystals in the bulk on substrates by physical adsorption plays an important role for the growth of zeolite films on substrates.

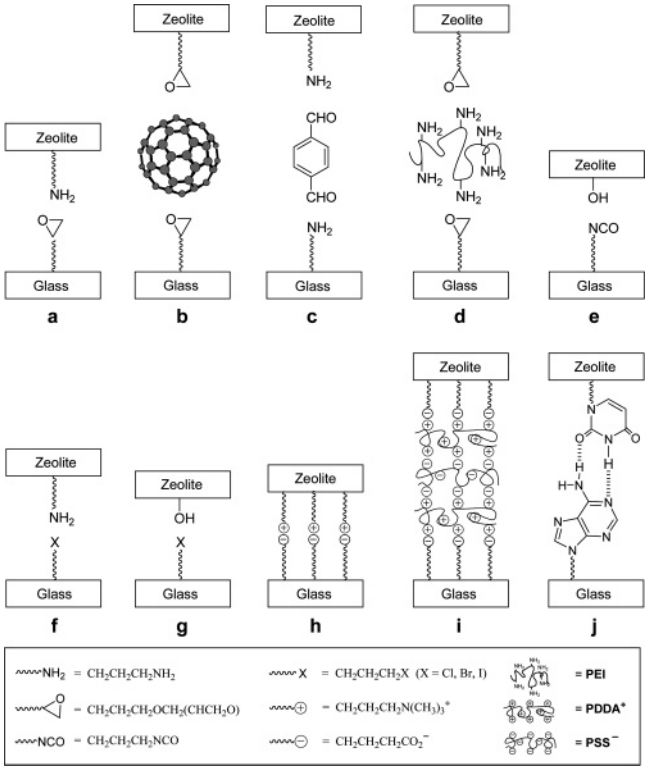

FIGURE 4. Various types of molecular linkages.

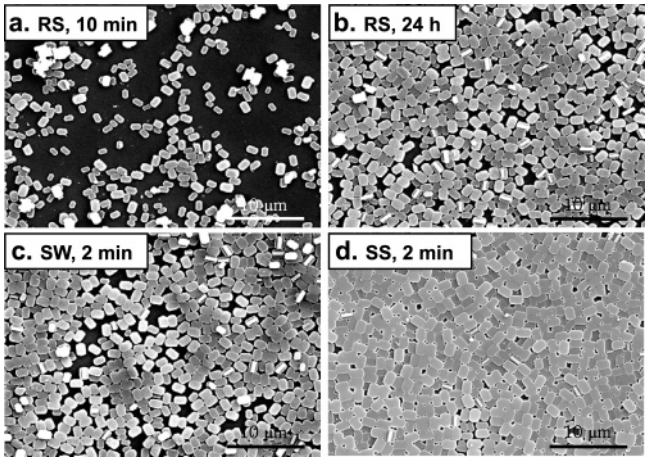

FIGURE 5. SEM images of bare silicalite crystal monolayers assembled on chloropropyl-tethering glass plates after reaction with reflux and stirring (RS) for 10 min (a) and 24 h (b), with sonication without stacking (SW) for 2 min (c), and with sonication with stacking (SS) for 2 min (d).[20]

Effect of Mode of Reaction Promotion on Rate, Close Packing, and Coverage

Mode of reaction promotion sensitively affects the above factors (Figure 5).[20] For instance, the rate of monolayer assembly increases in the order sonication with stacking ≥ sonication without stacking ≫ reflux and stirring. Best coverage and close packing were achieved by sonication with stacking for 2 min. The coverage and close packing achieved by sonication without stacking for 2 min were comparable with those achieved by reflux and stirring for 24 h.

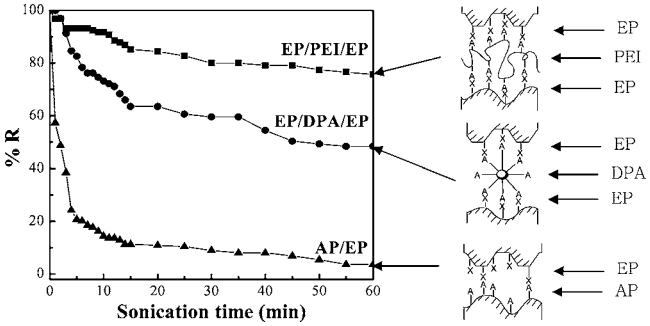

FIGURE 6. Plot of %*R* vs sonication time for the monolayers of zeolite-A crystals assembled on glass plates through AP/EP, EP/dendritic polyamine (DPA)/EP, and EP/polyethylene imine (PEI)/EP linkages.[8]

The sonication-induced dramatic increases in rate, coverage, and close packing are attributed to a large increase in the surface-migration rate of the substrate-bound crystals arising from large increases in the rates of bond breaking and bond reforming between the microcrystals and substrates. In the case of sonication with stacking, fast influx of zeolite particles from the bottom of the glass stacks to the top is attributed to dramatic increases because the influx inevitably 'pushes' the previously attached crystals to the top, giving rise to very tight lateral close packing between the crystals.[20]

Factors that Affect Binding Strength

The numbers of interconnecting linkages should be large to maintain strong adhesion between microcrystals and substrates. Over 660 000 linkages can be formed between an atomically flat $1 \times 1\ \mu m^2$ face of a zeolite microcrystal and a substrate.[8] However, the actual numbers of interconnecting linkage are much smaller due to surface unevenness of zeolites and substrates. For instance, the surface roughness of silicalite-1 was ~15 nm, which is much larger than the lengths of molecular linkers (~1 nm).[29]

Sonication-induced detachment of the glass-bound zeolite crystals in clean, zeolite-free toluene has been adopted as a qualitative measure for binding strengths.[8] For this, the percentage of the remaining amount of zeolite crystals after sonication for a certain period of time with respect to the initially attached amount (%*R*) was obtained and plotted with respect to sonication time. The following three methodologies lead to binding strength increase.

A. Use of Polymeric Linkers. Use of polyamines (dendritic polyamine or polyethyleneimine) as the intermediate linkers leads to a marked increase in binding strength (Figure 6), presumably due to their ability to position within the nanovalleys of the solid surfaces in such a way as to increase the amount of linkages between the two surfaces.[8]

Although ionic linkage gives rise to stronger binding strength (vide supra), use of polyelectrolytes and the increase in the number of polyelectrolyte layers further lead to a significant increase in binding strength.[9] By taking advantage of this, multilayer (pentalayer) assembly

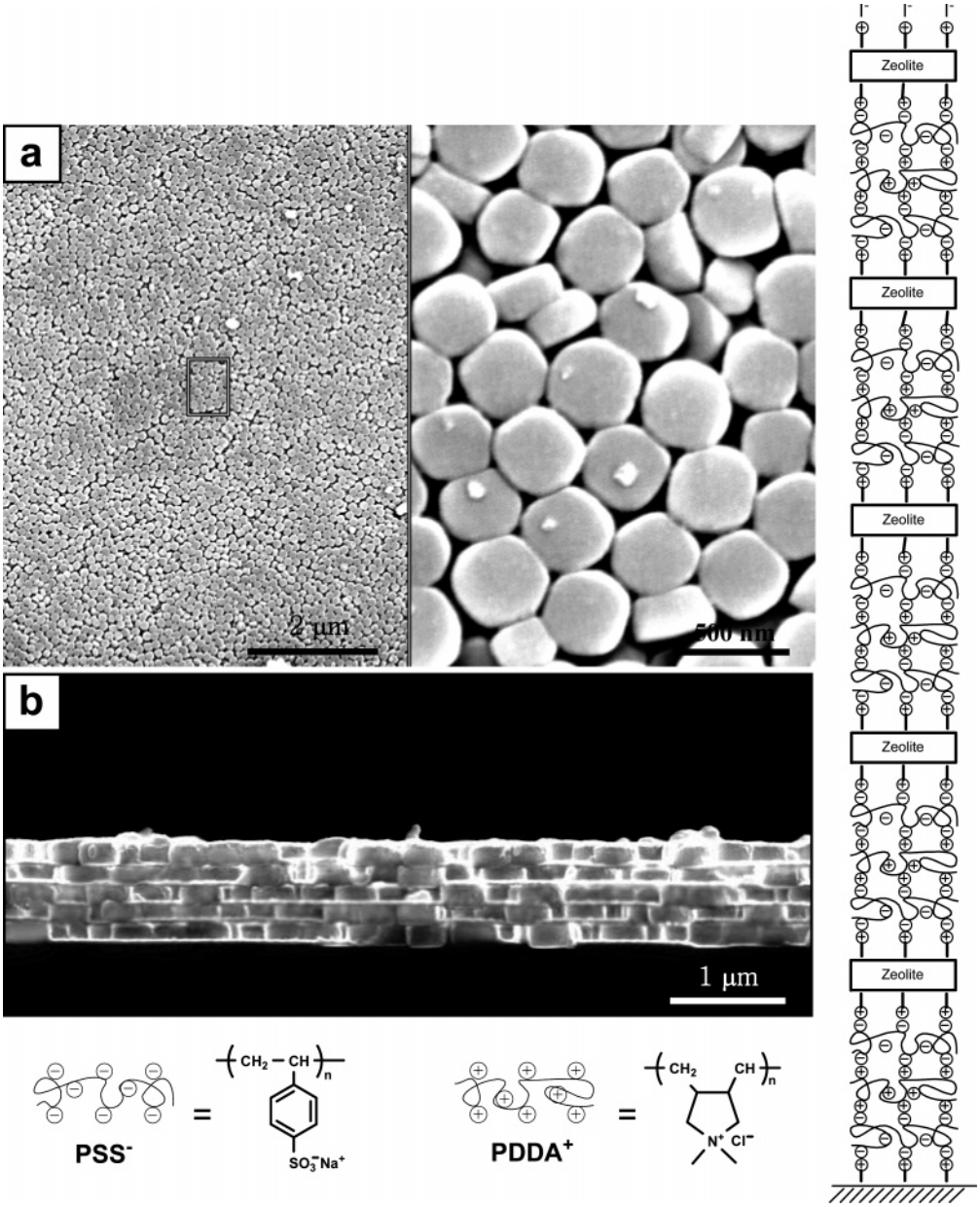

FIGURE 7. SEM images of a pentalayer of silicalite crystals assembled on a glass plate through ionic linkages with $PSS^-/PDDA^+/PSS^-$ as the intermediate linkers: top view (a) and cross section (b).[9]

of zeolite microcrystals on glass was successively carried out using $PSS^-/PDDA^+/PSS^-$ as the repeating linkage units (Figure 7).

B. Cross-Linking between the Adjacent Microcrystals. The lateral cross-linking between the neighboring, adjacent microcrystals leads to a marked increase in binding strength despite the fact that the amount of linkages between the microcrystals and the underlying glass substrate remained unaltered.[18] For instance, cross-linking of the neighboring aminopropyl-tethering cubic zeolite-A microcrystals with terephthaldicarboxaldehyde led to a 7-fold increase in binding strength (Figure 8). Such a phenomenon was more pronounced with decreasing crystal size.

C. Assembly with Strong Agitation. Under the condition of reflux and stirring, the kinetic energies of the functional groups tethered to microcrystals and substrates are very small due to very large masses of the host solids. Sonication-induced strong agitation of the microcrystals and substrates leads to a marked increase in binding strength. For instance, $\%R$ of the microcrystals attached to glass by sonication (with or without stacking) for 2 min was 60 times higher than those of the microcrystals that were attached to glass by reflux and stirring for 2 min.[20] Such a marked increase is attributed to the increase in amount of linkages arising from the increase in kinetic energies of the functional groups tethered to microcrystals and substrates, which facilitates their linkage formation reactions during collision between microcrystals and substrates.

Sonication induces detachment as well as attachment. This contradictory behavior of sonication suggests that it

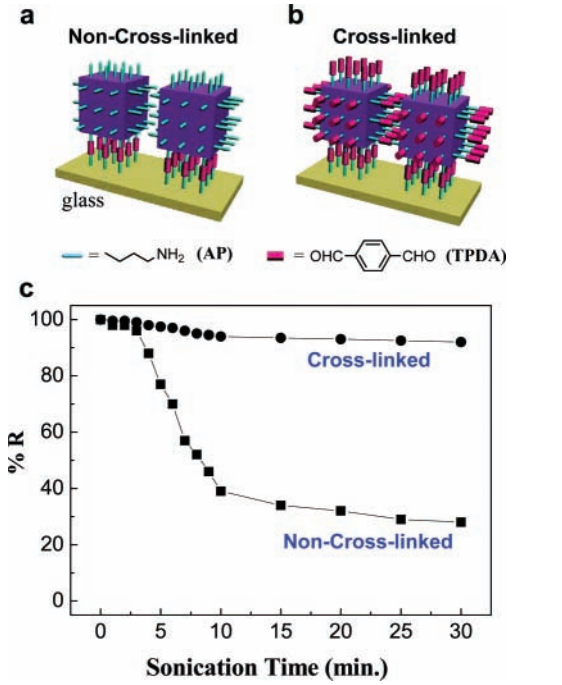

FIGURE 8. Illustration of non-cross-linking (a) and cross-linking (b) between the neighboring microcrystals, and plot of %*R* vs sonication time (c).[18]

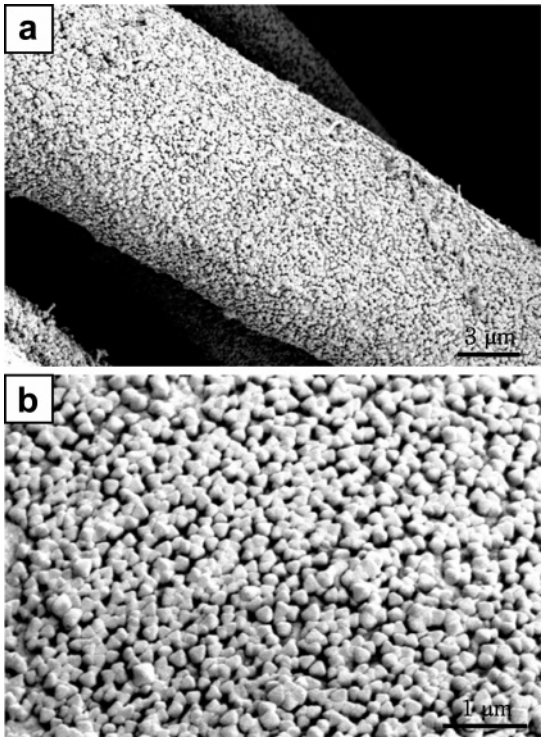

FIGURE 9. SEM images of a nano-zeolite-Y-coated cotton fiber.[11]

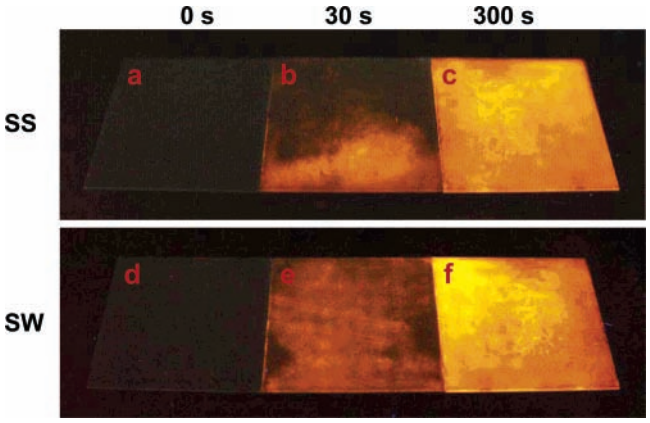

FIGURE 10. Luminescence images of the glass plates coated with a closely packed monolayer of bare silicalite crystals (SL/G) (a), after treatment with a fluorophore-incorporating silicalite for 30 (b) and 300 s (c), respectively, with sonication with stacking (SS) and the corresponding SL/Gs (d, e, f) with sonication without stacking (SW). λ_{ext} = 350 nm; fluoropore = *n*-nonylhemicyanine.[20]

could act as a selection procedure by which only the strongly attached crystals remain attached while the weakly attached crystals are detached. However, this does not explain the above large difference in binding strength after reaction for 2 min since detachment is not undergone extensively during such a short period. Furthermore, no crystals are detached from the substrate for 2 min in the case of sonication with stacking. The vibration-induced 'strong hitting' of the surface-bound microcrystals with side glass plates seems to give rise to the increase in binding strength.

Binding strength is a function of reaction period. With sonication, binding strength decreases after 1 h due to a gradual decrease in amount of linkage resulting from undergoing repeated bond breaking and bond reforming. With reflux and stirring, the binding strength of the microcrystals gradually increased during the period from 0 to 18 h, indicating that the amount of linkage increases during the period.

D. Calcination. The binding strength between microcrystals and glass substrates increases dramatically when the microcrystal-bound glass plates were calcined at 350−450 °C for 3−4 h to remove organic linkages, presumably due to formation of direct Si−O−Si linkages between the zeolite microcrystals and the substrates during calcination.

Types of Substrates

The substrates that have been tested so far are glass,[2,3,5,8−10,12,15−22] glass fiber,[8] silica,[4] alumina,[4] large zeolite,[4] vegetable fibers (cotton, linen, and hemp) (Figure 9),[11] artificial fibers (nylon and polyester), and conducting substrates (Pt, Au, and ITO glass).[19]

Replacement of Attached Crystals with Those Dispersed in Solution and Surface Migration of Attached Crystals

Glass-bound bare zeolite microcrystals were readily replaced by the fluorophore-incorporating zeolite microcrystals dispersed in solution (Figure 10), indicating that the substrate-bound microcrystals are continuously replaced by those dispersed in solution.[20] The rate increased with increasing the degree of agitation. The substrate-bound zeolite microcrystals readily move around on the surface during monolayer assembly.[20] In the case of reflux and stirring, the solvent bubbles generated from the

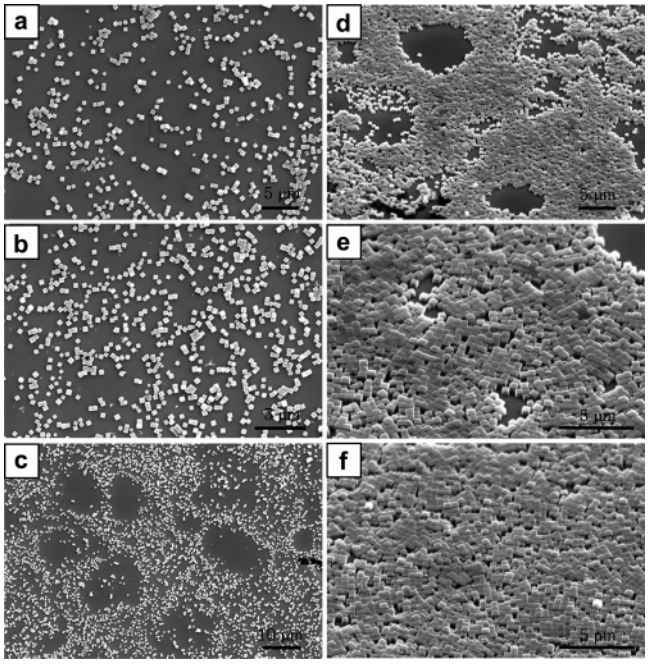

FIGURE 11. SEM images of various spots on a glass plate showing different degrees of coverage during monolayer assembly with zeolite-A crystals.[3]

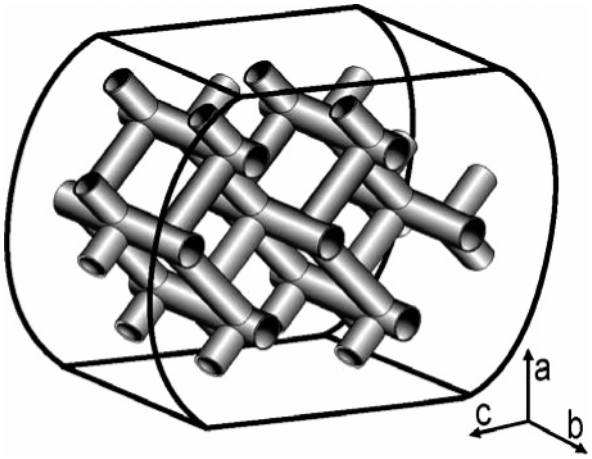

FIGURE 12. Orientations of a silicalite crystal and its channels.[16]

substrate-bound crystals help their surface migration as shown in Figure 11.[3]

Driving Force for Uniform Orientation

Silicalite-1 crystals can be attached to substrates in two orientations, *a*-orientation and *b*-orientation (Figure 12), that is, *a* and *b* axes pointing normal to the substrate, respectively. *b*-Orientation is most prevalent (>99%), and *a*-orientation is found only during the initial stages. The reasons that lead to high degrees of uniform orientation are as follows. First, the attached crystals are continuously replaced by those dispersed in solution. Second, the binding strength between each microcrystal and substrate increases with increasing contact area. Consequently, the probability of a substrate-bound microcrystal to be replaced by those in solution decreases when attached through the largest area face. Thus, the largest area face

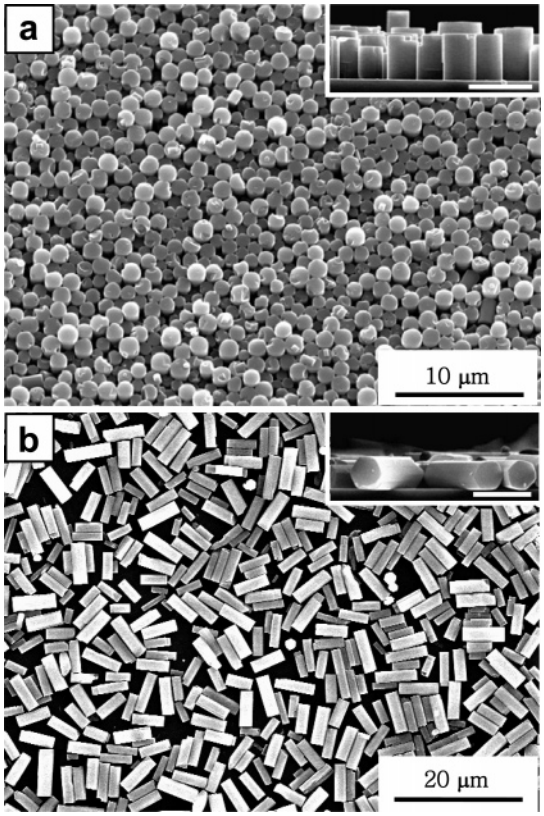

FIGURE 13. Monolayers of closely packed and vertically aligned cylindrical zeolite-L crystals (a) and horizontally aligned hexagonal columnar zeolite-L crystals (b) assembled on a 3-chloropropyl-tethering glass plate. Insets show cross sections; scale bar = 2 μm.[21]

determines the orientation of the attached crystals. This phenomenon is responsible for formation of *b*-oriented continuous films on substrates during silicalite-1 film growth.[33]

The cylindrical zeolite-L crystals formed vertically oriented monolayers (Figure 13a), while hexagonal columnar zeolite-L crystals formed horizontally oriented monolayers (Figure 13b).[21] The former occurs because the crystals have flat faces only at the bases, and the latter occurs because the areas of the side planes are significantly larger than those of basal planes. The methods to synthesize flat-faceted zeolite-L in two different morphologies are described in our recent report.[34]

Mode of reaction promotion also affects the degree of uniform orientation. For instance, the degree of vertical orientation of cylindrical zeolite-L crystals with the aspect ratio > 2 increases in the order reflux and stirring < sonication without stacking ≪ sonication with stacking. When the aspect ratio is less than 1, sonication without stacking also readily produces monolayers of *c*-oriented crystals.[35]

Electric field-driven alignment of long ZSM-5 crystals was demonstrated.[36] This physical method is limited to those crystals having net sizable intrinsic dipole moments. Growth of vertically oriented aluminophosphate molecular sieves using anodized alumina discs was also demonstrated.[37] However, the degrees of coverage, close packing,

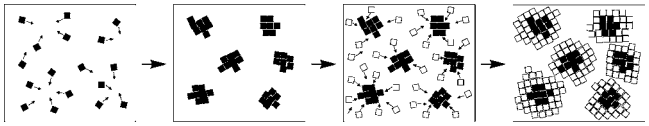

FIGURE 14. Illustration of close packing of zeolite microcrystals through surface migration on the substrate.[3]

and uniform orientation cannot compete with those shown in Figure 13a.

Driving Force for Close Packing

During monolayer assembly with hydrogen bonding, the weak hydrogen-bonding and hydrophobic interaction between the surface-tethered thymine groups seems to be the driving force for close packing. During monolayer assembly of bare or functional-group-tethering microcrystals in toluene or in ethanol, the hydrophilic interaction between the crystals in the relatively hydrophobic solvent seems to be an important contribution.

Factors that Affect Close Packing

Surface migration of attached crystals is an important factor for close packing. Figure 14 illustrates the proposed mechanism: initial random attachment of the crystals, surface migration leading to close packing, and subsequent random attachment.[3] For close packing to occur, the crystals should repeatedly undergo the cycle of bond breaking between the existing linkages and bond forming between the new, undamaged functional groups. Therefore, close packing becomes easier with decreasing binding strength (covalent bonding < amine-metal bonding < H-bonding; Figure 15) and increasing degree of agitation.

Patterned Monolayer Assembly

Micropatterned monolayers of zeolite microcrystals have the potential to be applied as combinatorial catalysts and low-dielectric packing materials for integrated circuits.[38,39] The first step is preparation of micropatterned monolayers of functional groups on substrates using microcontact printing[5] or photopatterning.[10,22] Figure 16a illustrates a microcontact printing-based procedure. A typical SEM image of a micropatterned monolayer of ZSM-5 crystals is shown in Figure 17a. The related micropatterned microporous and mesoporous silica films were prepared by Stucky, Yan, Zhao, Ozin, and co-workers.[40−42]

Photochemical degradation of organic linker groups tethered to glass surfaces is a highly versatile and effective way for preparing glass plates patterned with organic linker groups.[10] Thus, when a 3-halopropyl-tethering glass plate was exposed to UV light under a photomask, the UV-exposed halopropyl groups were selectively degraded (Figure 16b). While 3-halopropyl-tethering crystals formed monolayers only on the UV-exposed areas (Figure 17b), the bare crystals formed monolayers only on the unexposed areas (Figure 17c).

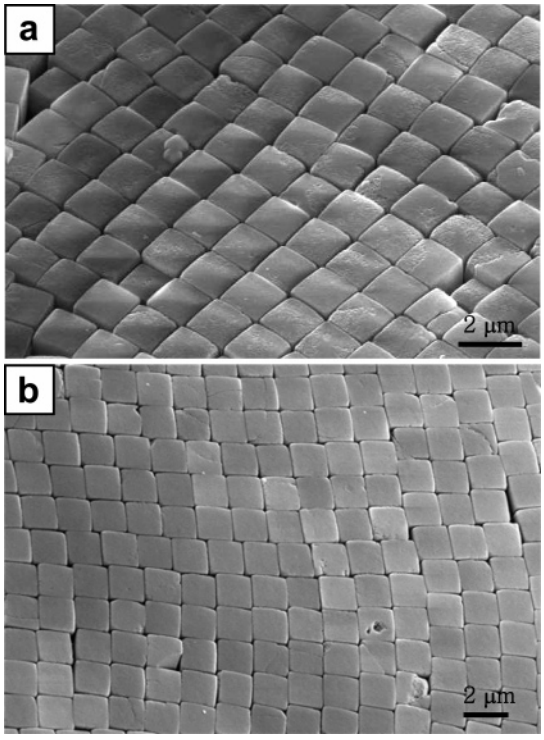

FIGURE 15. Monolayer of thymine-tethering zeolite-A microcrystals assembled on an adenine-tethering glass plate (a), and monolayer of aminopropyl-tethering zeolite-A monolayers assembled on platinum (b).[12,15]

Patterned continuous silicalite-1 films are obtained by immersing photopatterned glass plates into the corresponding synthesis gel.[10] The weaker attractive force between the colloidal seed crystals and gold was also utilized to produce patterned continuous silicalite-1 films on silicon wafers.[38] Photoinduced decarboxylation of glass-bound silver butyrate ($C_3H_7-CO_2^-Ag^+$) is an efficient way for micropatterned monolayer assembly of zeolite microcrystals on substrates through ionic linkages.[22]

Synthesis of Zeolite as Ordered Multi-Crystal Arrays

Monolayer assembly of zeolite crystals does not allow us to freely control the orientation of attached zeolite crystals since it is determined by the largest area face. Stemming from the facile transformation of polyurethane sponges into self-supporting silicalite-1 foams,[43,44] we discovered that uniformly aligned polyurethane films serve as templates for orientation-controlled synthesis of 2D and 3D arrays of silicalite-1 crystals, where the crystal orientation is controlled by varying the nature of polyurethane.[16]

For this, we prepared glass plates coated with 500 layers of uniformly aligned poly-(PDI/BDO) [$(PDI/BDO)_{500}$/G] and poly-[PDI/TBE] [$(PDI/TBE)_{500}$/G] (Figure 18). When the hydrothermal reaction of silicalite-1 was carried out in the presence of $(PDI/BDO)_{500}$/G, closely packed 2D arrays of *c*-oriented silicalite-1 crystals covered the glass substrates (Figure 19a). There were some areas covered with second layers of *c*-oriented crystals (Figure 19b), indicating that production of even 3D arrays of uniformly

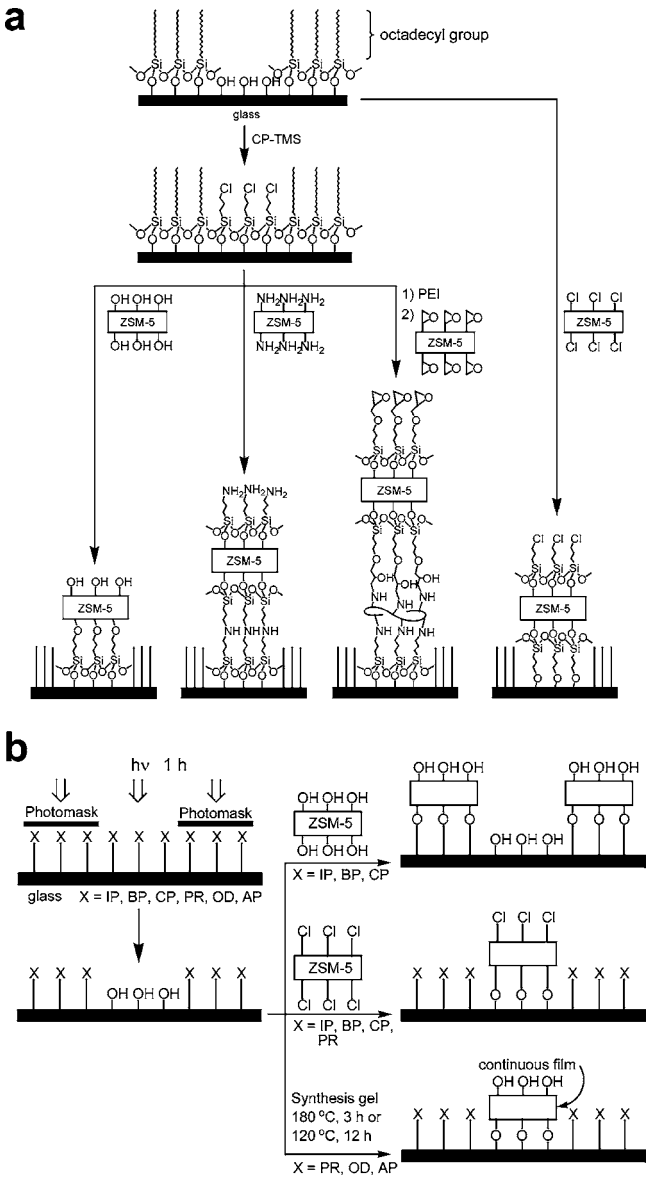

FIGURE 16. Schematic procedures for the microcontact-based micropatterned monolayer assembly of zeolite microcrystals on glass (a) and for photochemical methods for micropatterned monolayer assembly of microcrystals or direct growth of continuous zeolite films on glass (b).[5,10]

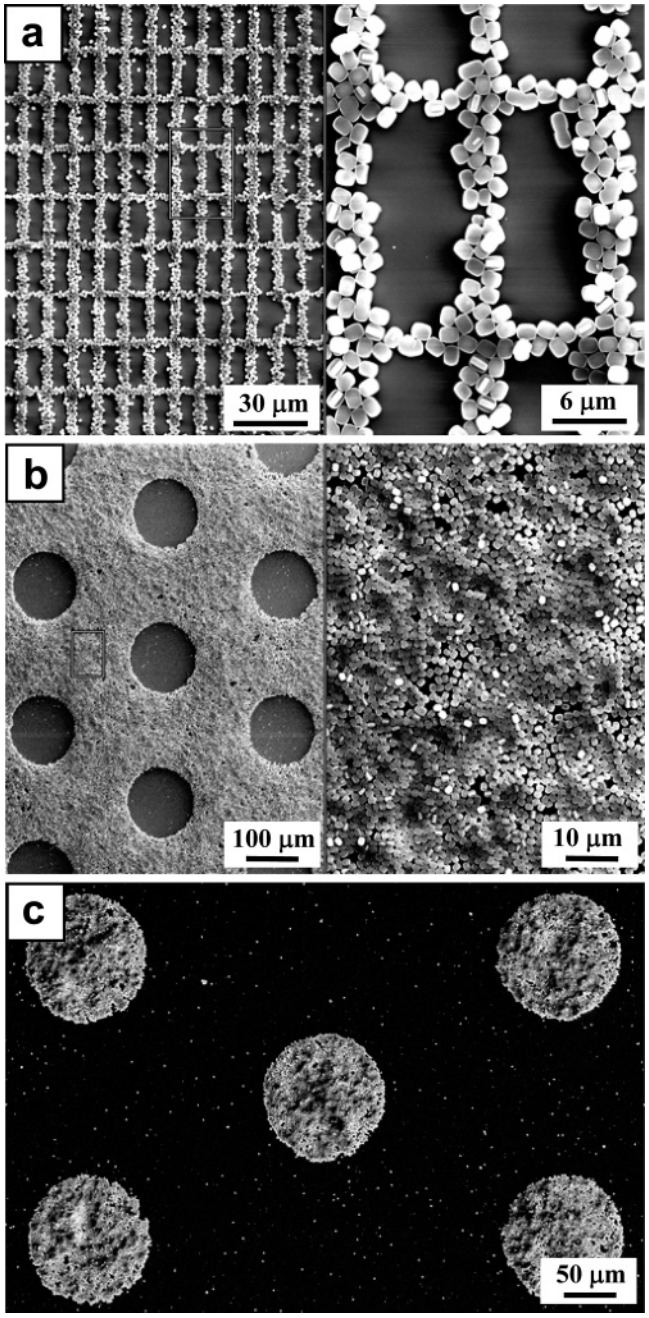

FIGURE 17. SEM images of micropatterned monolayers of zeolite microcrystals.[5,10]

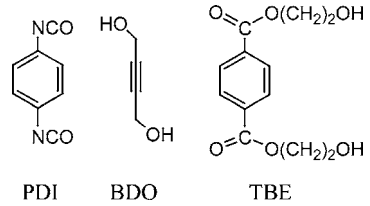

FIGURE 18. Structures of phenylene diisocyanate (PDI), 2-butyne-1,4-diol (BDO), and terephthalic acid bis-(2-hydroxy ethyl) ester (TBE).

aligned silicalite-1 crystals is also possible by optimization of the condition. In strong contrast, only *b*-oriented silicalite-1 crystals grew on bare glass plates in the same gel. Randomly oriented poly(PDI-BDO) fibers gave only randomly aggregated crystals.

In the case of $[(PDI/TBE)_{500}/G]$, closely packed 2D arrays of *a*-oriented silicalite-1 crystals covered the glass substrates (Figure 19c). Supramolecular organization of the hydrolyzed organic products and the reactive silicon species seems to be responsible for the above phenomenon. We originally proposed that nanoslabs[45] were the reactive silicon species. However, the disproval of the existence of nanoslabs[46,47] suggests that systematic intensive research is necessary to elucidate the mechanism of the above highly intriguing phenomenon.

The organic species in synthesis gels (such as TPA^+) have been known as 'structure directors' for creation of nanopores in certain shapes, sizes, and networks in zeolites. Our result indicates that the organic species can also serve as 'orientation directors' for the produced

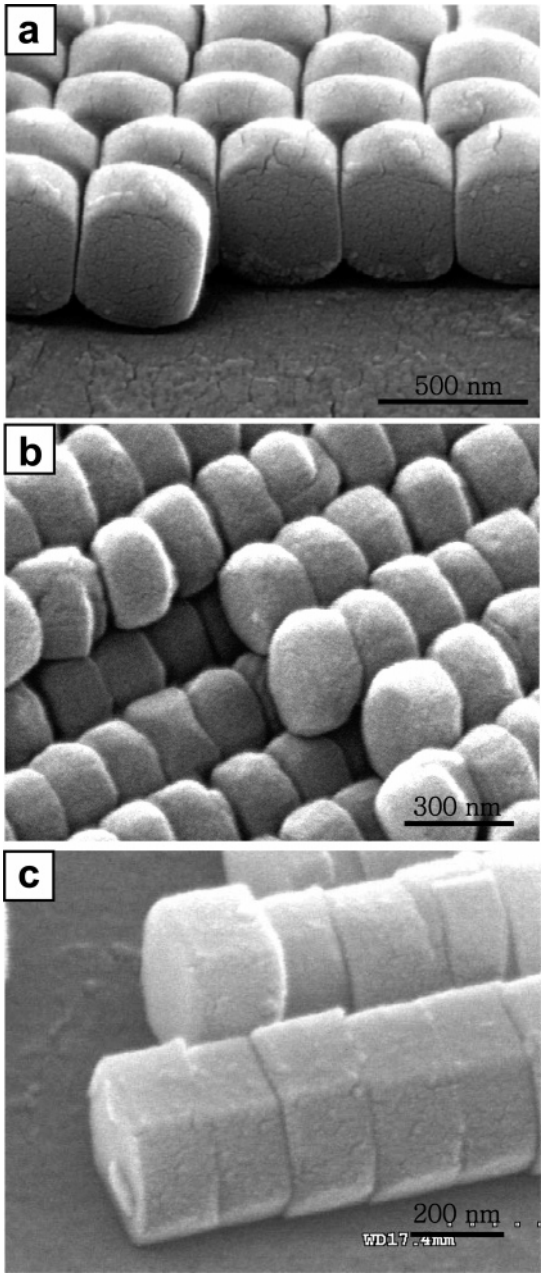

FIGURE 19. Monolayer (a) and double layer (b) of closely packed, *c*-oriented silicalite-1 crystals grown on $(PDI/BDO)_{500}/G$, and a monolayer of closely packed *a*-oriented silicalite-1 crystals grown on $(PDI/TBE)_{500}/G$ (c).[16]

crystals. Bein and co-workers reported the growth of randomly scattered zincophosphate and $AlPO_4$-5 crystals in certain orientations on alkyl phosphate-coated gold.[48]

Preparation of Surface-Aligned Zeolite Microballs

Zeolite nanocrystals (150 nm) can be organized into self-supporting zeolite microballs (1−20 μm) by adding a small amount of water into a toluene solution predispersed with zeolite nanocrystals followed by vigorous sonication.[14] The water droplets dispersed in toluene acted as templates to attract hydrophilic zeolite crystals (Figure 20a). The developed strong bonding between the bare zeolite nanocrystals suggests that direct siloxyl linkages form between the nanocrystals during sonication by undergoing dehydration reaction between the surface hydroxyl groups.

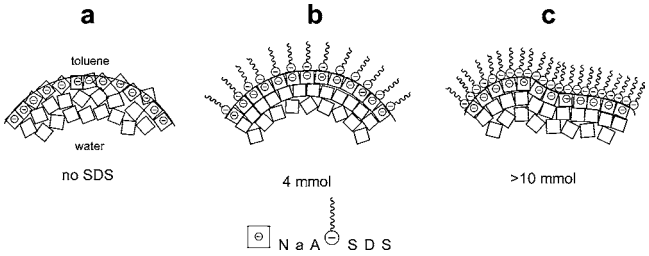

FIGURE 20. Illustrations of a water droplet in toluene acting as a template to attract hydrophilic zeolite crystals (a) and the aligned anionic surfactant molecules (sodium dodecylsulfate, SDS) acting as nanotools for the alignment of zeolite-A crystals at the water−toluene interface at an intermediate concentration of SDS (b), and a deformed structure of a water pool caused by high concentrations of SDS (c).[14]

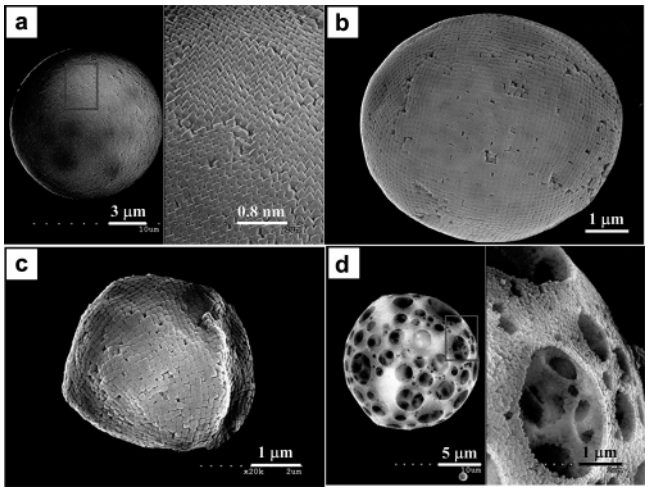

FIGURE 21. SEM images of a microball composed of octahedral zeolite-X crystals (size = ∼150 nm) and its uniformly aligned surface (a), an egg-shaped ball composed of cubic zeolite-A crystals (size = ∼150 nm) and its uniformly aligned surface (b), a highly deformed ball with aligned surface (c), and a perforated ball showing the 3D network of voids (d).[14]

When produced from pure water, the microballs consisted of randomly oriented nanocrystals (Figure 20a). Sodium dodecylsulfate induces the zeolite nanocrystals in the two outermost surface layers of microballs uniformly aligned (Figures 20b and 21a,b). The following may explain the above phenomenon. Dodecylsulfate ions self-assemble at the water−toluene interface with the negatively charged polar heads pointing to water droplets (Figure 20b). To minimize electrostatic repulsion with the negative heads, zeolite nanocrystals uniformly align in such a way as to minimize surface area. At higher concentrations of dodecylsulfate, the zeolite nanocrystals assembled into anisotropic structures (Figures 20c and 21c) due to the decrease of the surface energy.

Perforated zeolite microballs were produced during the initial periods of sonication (Figure 21d). The shaded spots in Figure 21a represent the internal voids covered with thin layers (usually monolayers) of zeolite. The 3D net-

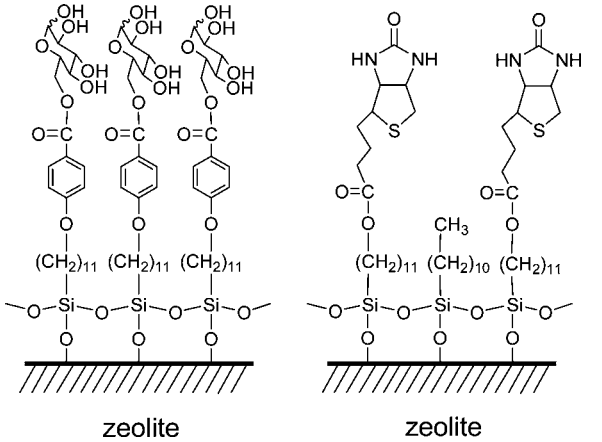

FIGURE 22. Zeolite-A microcrystals tethering β-D-glucose (a) and biotin (b) groups.[7,13]

works of the perforated spherulites can be seen from Figure 21d (right).

The above methodology can be applied to organize nonspherical nanoparticles in high ordering. The highly perforated microballs of zeolite nanocrystals can be utilized as highly effective catalysts and adsorbents. The microballs also show the anatomies of emulsions.

Self-Assembly of Substrate-Tethering Zeolite Crystals with Proteins

Examples of self-assembly of substances into structured aggregates, in particular by enzyme−substrate complexation, are very rare. We discovered a novel phenomenon that β-glucosidase and D-glucose-tethering zeolite microcrystals (Figure 22a) and avidin and D-biotin-tethering zeolite microcrystals (Figure 22b) readily self-assemble into thin (2−20 μm) and long (>1 cm) fibrils (Figure 23a,b) upon stirring them in aqueous buffer solutions at which the protein activities are highest.[7,13] The morphology of the fibrils is sensitively governed by the protein/zeolite ratio. In the case of avidin and D-biotin-tethering zeolite microcrystals, discrete clusters of zeolite crystals with sizes of 5−10 μm (Figure 23c) are produced when the protein/zeolite = 0.1.

The above results represent an unprecedented phenomenon that a protein and its substrate-tethering inorganic microcrystals self-assemble into structured aggregates. Although the mechanism is unclear, in particular as to why the two components grow into axial symmetry, this method is a way to organize zeolite microcrystals with protein.

Current and Future Applications

The uniformly aligned zeolite monolayers can be immediately used as excellent precursors for molecular sieve membranes.[49] They can also be used to characterize paramagnetic species in zeolites.[17] The natural and synthetic fabrics and papers coated with Ag^+-exchanged zeolite crystals can be used as novel antibacterial functional fabrics and papers.[11] The optical fibers coated with

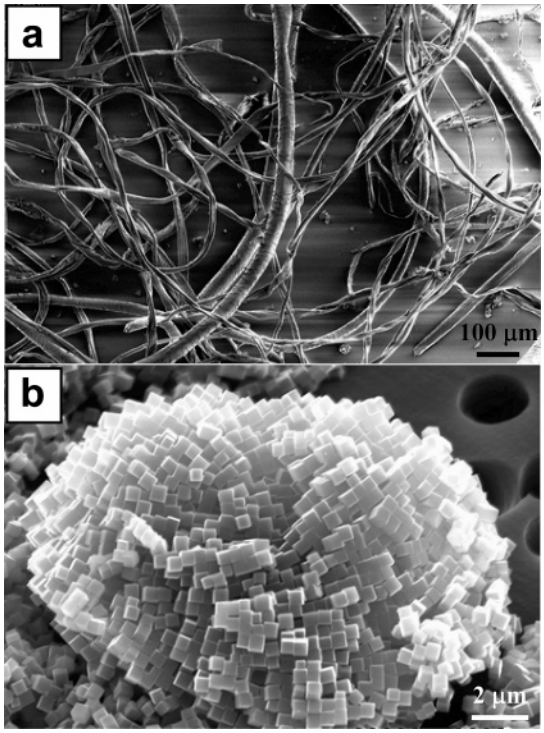

FIGURE 23. SEM images showing the fibrous zeolite-A-β-D-glucosidase composite material (a) and a discrete cluster of biotin-tethering zeolite-A crystals (b).[7,13]

zeolite microcrystals can be used as high-efficiency photocatalysts.[50] The monolayers of vertically oriented fluorophore-incorporating cylindrical zeolite-L crystals gave anisotropic photoluminescence (dichroic ratio = 8.9),[21] which is higher than the previously reported value (4.5) from the fluorescent polymer-incorporating mesoporous silica.[51] Thus, the uniformly aligned mono- and multilayers of zeolite crystals can also be used as media for generation of anisotropic photoluminescence,[21] supramolecularly organized light-harvesting systems,[35,52] and nonlinear optical films.[53] The micropatterned monolayers can be used as high-throughput combinatorial catalysts and low-dielectric packing materials for integrated circuits.[38,39] The highly perforated microballs of zeolite nanocrystals can be utilized as effective catalysts and adsorbents. Although the assembly of zeolite microcrystals into 3D supercrystals is still a challenge, we believe that this is the direction to which the zeolite microcrystal organization should move since the resulting supercrystals could find many important optical and other applications. The zeolite microcrystal organization has been regarded as one of the future directions of zeolite research.[54,55]

Conclusion and Future Directions

The microbuilding blocks can be readily organized into 2D and 3D functional entities. The chemistry of microcrystals is doable and a highly promising area. We believe our findings set a new direction to which zeolite research should move, which will help zeolites be applied as innovative materials and devices.

I thank the graduate students and postdoctoral fellows whose names appear in the references for their hard work which made this Account possible and the Ministry of Science and Technology of Korea and Sogang University for financial support.

References

(1) (a) Bowden, N. B.; Weck, M.; Choi, I. S.; Whitesides, G. M. Molecule-mimetic chemistry and mesoscale self-assembly. *Acc. Chem. Res.* **2001**, *34*, 231−238. (b) Ozin, G. A. Panoscopic materials: synthesis over 'all' length scales. *Chem. Commun.* **2000**, 419−432.

(2) Kulak, A.; Lee, Y.-J.; Park, Y. S.; Yoon, K. B. Orientation-controlled monolayer assembly of zeolite crystals on glass and mica by covalent linkage of surface-bound epoxide and amine groups. *Angew. Chem., Int. Ed.* **2000**, *39*, 950−953.

(3) Choi, S. Y.; Lee, Y.-J.; Park, Y. S.; Ha, K.; Yoon, K. B. Monolayer assembly of zeolite crystals on glass with fullerene as the covalent linker. *J. Am. Chem. Soc.* **2000**, *122*, 5201−5209.

(4) Ha, K.; Lee, Y.-J.; Lee, H. J.; Yoon, K. B. Facile assembly of zeolite monolayers on glass, silica, alumina, and other zeolites using 3-halopropylsilyl reagents as covalent linkers. *Adv. Mater.* **2000**, *12*, 1114−1117.

(5) Ha, K.; Lee, Y.-J.; Jung, D. Y.; Lee, J. H.; Yoon, K. B. Micropatterning of oriented zeolite monolayers on glass by covalent linkage. *Adv. Mater.* **2000**, *12*, 1614−1617.

(6) Lee, G. S.; Lee, Y.-J.; Ha, K.; Yoon, K. B. Orientation-controlled monolayer assembly of zeolite crystals on glass using terephthaldicarboxaldehyde as a covalent linker. *Tetrahedron* **2000**, *56*, 6965−6968.

(7) Lee, G. S.; Lee, Y.-J.; Choi, S. Y.; Park, Y. S.; Yoon, K. B. Self-assembly of beta-glucosidase and D-glucose-tethering zeolite crystals into fibrous aggregates. *J. Am. Chem. Soc.* **2000**, *122*, 12151−12157.

(8) Kulak, A.; Park, Y. S.; Lee, Y.-J.; Chun, Y. S.; Ha, K.; Yoon, K. B. Polyamines as strong molecular linkers for monolayer assembly of zeolite crystals on flat and curved glass. *J. Am. Chem. Soc.* **2000**, *122*, 9308−9309.

(9) Lee, G. S.; Lee, Y.-J.; Yoon, K. B. Layer-by-layer assembly of zeolite crystals on glass with polyelectrolytes as ionic linkers. *J. Am. Chem. Soc.* **2001**, *123*, 9769−9779.

(10) Ha, K.; Lee, Y.-J.; Chun, Y. S.; Park, Y. S.; Lee, G. S.; Yoon, K. B. Photochemical pattern transfer and patterning of continuous zeolite films on glass by direct dipping in synthesis gel. *Adv. Mater.* **2001**, *13*, 594−596.

(11) Lee, G. S.; Lee, Y.-J.; Ha, K.; Yoon, K. B. Preparation of flexible zeolite-tethering vegetable fibers. *Adv. Mater.* **2001**, *13*, 1491−1495.

(12) Park, J. S.; Lee, G. S.; Lee, Y.-J.; Park, Y. S.; Yoon, K. B. Organization of microcrystals on glass by adenine-thymine hydrogen bonding. *J. Am. Chem. Soc.* **2002**, *124*, 13366−13367.

(13) Um, S. H.; Lee, G. S.; Lee, Y.-J.; Koo, K. K.; Lee, C.; Yoon, K. B. Self-assembly of avidin and D-biotin-tethering zeolite microcrystals into fibrous aggregates. *Langmuir* **2002**, *18*, 4455−4459.

(14) Kulak, A.; Lee, Y. J.; Park, Y. S.; Kim, H. S.; Lee, G. S.; Yoon, K. B. Anionic surfactants as nanotools for the alignment of nonspherical zeolite nanocrystals. *Adv. Mater.* **2002**, *14*, 526−529.

(15) Chun, Y. S.; Ha, K.; Lee, Y.-J.; Lee, J. S.; Kim, H. S.; Park, Y. S.; Yoon, K. B. Diisocyanates as novel molecular binders for monolayer assembly of zeolite crystals on glass. *Chem. Commun.* **2002**, 1846−1847.

(16) Lee, J. S.; Lee, Y.-J.; Tae, E. L.; Park, Y. S.; Yoon, K. B. Synthesis of zeolite as ordered multicrystal arrays. *Science* **2003**, *301*, 818−821.

(17) So, H.; Ha, K.; Lee, Y.-J.; Yoon, K. B.; Belford, R. L. Observation of single-crystal-type EPR spectra from monolayers of copper-exchanged zeolite Na-A crystals assembled on glass plates. *J. Phys. Chem. B* **2003**, *107*, 8281−8284.

(18) Park, J. S.; Lee, Y.-J.; Yoon, K. B. Marked increase in the binding strength between the substrate and the covalently attached monolayers of zeolite microcrystals by lateral molecular cross-linking between the neighboring microcrystals. *J. Am. Chem. Soc.* **2004**, *126*, 1934−1935.

(19) Ha, K.; Park, J. S.; Oh, K. S.; Zhou, Y. S.; Chun, Y. S.; Lee, Y.-J.; Yoon, K. B. Aligned monolayer assembly of zeolite crystals on platinum, gold, and indium-tin oxide surfaces with molecular linkages. *Microporous Mesoporous Mater.* **2004**, *72*, 91−98.

(20) Lee, J. S.; Ha, K.; Lee, Y.-J.; Yoon, K. B. Ultrasound-aided remarkably fast assembly of monolayers of zeolite crystals on glass with a very high degree of lateral close packing. *Adv. Mater.* **2005**, *17*, 837−841.

(21) Lee, J. S.; Lim, H.; Ha, K.; Cheong, H.; Yoon, K. B. Facile monolayer assembly of fluorophore-incorporating zeolite rolds in uniform orientations for anisotropic photoluminescence. *Angew. Chem., Int. Ed.* **2006**, *45*, 5288−5292.

(22) Park, J. S.; Lee, G. S.; Yoon, K. B. Micropatterned monolayer assembly of zeolite microcrystals on glass by ionic linkages. *Microporous Mesoporous Mater.* **2006**, *96*, 1−8.

(23) Li, Z.; Lai, C.; Mallouk, T. E. Self-assembling trimolecular redox chains at zeolite Y modified electrodes. *Inorg. Chem.* **1989**, *28*, 178−182.

(24) Yan, Y.; Bein, T. Molecular recognition on acoustic wave devices: sorption in chemically anchored zeolite monolayers. *J. Phys. Chem.* **1992**, *96*, 9387−9393.

(25) Li, J.-W.; Pfanner, K.; Calzaferri, G. Silver-zeolite-modified electrodes: An intrazeolite electron transport mechanism. *J. Phys. Chem.* **1995**, *99*, 2119−2126.

(26) Mintova, S.; Schoeman, B.; Valtchev, V.; Sterte, J.; Mo, S.; Bein, T. Growth of silicalite films on pre-assembled layers of nanoscale seed crystals on piezoelectric chemical sensors. *Adv. Mater.* **1997**, *9*, 585−589.

(27) Boudreau, L. C.; Kuck, J. A.; Tsapatsis, M. Deposition of oriented zeolite A films: in situ and secondary growth. *J. Membr. Sci.* **1999**, *152*, 41−59.

(28) Yoon, K. B. Mono and multilayer assembly of zeolite microcrystals on substrates. *Bull. Korean Chem. Soc.* **2006**, *27*, 17−26. In the case of zeolite-A (unit cell = 2.461 nm), there are 164 973 unit cells in 1 μm^2. Since each unit area (2.461^2 nm^2) carries four S4R rings and each S4R ring can tether at least one functional group using four OH groups, the minimum number of attachable functional groups per 1 μm^2 is 659 894. Multiplication of the number by 4 gives 2 639 577. The actual number should be much smaller due to surface unevenness (ref 29).

(29) Lee, H.; Park, J. S.; Kim, H.; Yoon, K. B.; Seeck, O. H.; Kim, D. H.; Seo, S. H.; Kang, H. C.; Noh, D. Y. Characterization of molecular linkages placed between zeolite microcrystal monolayers and a0 substrate with X-ray reflectivity. *Langmuir* **2006**, *22*, 2598−2604.

(30) Lainé, P.; Seifert, R.; Giovanoli, R.; Calzaferri, G. Convenient preparation of close-packed monograin layers of pure zeolite A microcrystals. *New J. Chem.* **1997**, *21*, 453−460.

(31) Lee, J. A.; Meng, L.; Norris, D. J.; Scriven, L. E.; Tsapatsis, M. Colloidal crystal layers of hexagonal nanoplates by convective assembly. *Langmuir* **2006**, *22*, 5217−5219.

(32) Ban, T.; Ohwaki, T.; Ohya, Y.; Takahashi, Y. Preparation of a completely oriented molecular sieve membrane. *Angew. Chem., Int. Ed.* **1999**, *38*, 3324−3326.

(33) Li, S.; Li, Z.; Bozhilov, K. N.; Chen, Z.; Yan, Y. TEM investigation of formation of monocrystal-thick b-oriented pure silica zeolite MFI film. *J. Am. Chem. Soc.* **2004**, *126*, 10732−10737.

(34) Lee, Y.-J.; Lee, J. S.; Yoon, K. B. Synthesis of long zeolite-L crystals with flat facets. *Microporous Mesoporous Mater.* **2005**, *80*, 237−246.

(35) Ruiz, A. Z.; Li, H.; Calzaferri, G. Organizing supramolecular functional dye-zeolite crystals. *Angew. Chem., Int. Ed.* **2006**, *45*, 5282−5287.

(36) Caro, J.; Finger, G.; Kornatowski, J.; Richter-Mendau, J.; Werner, L.; Zibrowius, B. Aligned molecular sieve crystals. *Adv. Mater.* **1992**, *4*, 273−276.

(37) Tsai, T. G.; Shih, H. C.; Liao, S. J.; Chao, K. J. Well-aligned SAPO-5 membrane: preparation and characterization. *Microporous Mesoporous Mater.* **1998**, *22*, 333−341.

(38) Li, S.; Demmelmaier, C.; Itkis, M.; Liu, Z.; Haddon, R. C.; Yan, Y. Micropatterned oriented zeolite monolayer films by direct in situ crystallization. *Chem. Mater.* **2003**, *15*, 2687−2689.

(39) Wang, Z.; Mirta, A.; Wang, H.; Huang, L.; Yan, Y. Pure-silica zeolite films as low-k dielectrics by spin-on of nanoparticle suspensions. *Adv. Mater.* **2001**, *13*, 1463−1466.

(40) Yang, P.; Deng, T.; Zhao, D.; Feng, P.; Pine, D.; Chmelka, B. F.; Whitesides, G. M.; Stucky, G. D. Hierarchically ordered oxides. *Science* **1998**, *282*, 2244−2246.

(41) Huang, L.; Wang, Z.; Sun, J.; Miao, L.; Li, Q.; Yan, Y.; Zhao, D. Fabrication of ordered porous structures by self-assembly of zeolite nanocrystals. *J. Am. Chem. Soc.* **2000**, *122*, 3530−3531.

(42) Yang, H.; Coombs, N.; Ozin, G. A. Mesoporous silica with micrometer-scale designs. *Adv. Mater.* **1997**, *9*, 811−814.

(43) Lee, Y.-J.; Lee, J. S.; Park, Y. S.; Yoon, K. B. Synthesis of large monolithic zeolite foams with variable macropore architectures. *Adv. Mater.* **2001**, *13*, 1259−1263.

(44) Lee, Y.-J.; Yoon, K. B. Effect of composition of polyurethane foam template on the morphology of silicalite foam. *Microporous Mesoporous Mater.* **2005**, *88*, 176−186.

(45) Kirschhock, C. E. A.; Buschmann, V.; Kremer, S.; Ravishankar, R.; Houssin, C. J. Y.; Mojet, B. L.; van Santen, R. A.; Grobet, P. J.; Jacobs, P. A.; Martens, J. A. Zeosil nanoslabs: building blocks in nPr_4N^+-mediated synthesis of MFI zeolite. *Angew. Chem., Int. Ed.* **2001**, *40*, 2637−2640.
(46) Cheng, C.-H.; Shantz, D. F. ^{29}Si NMR studies of zeolite precursor solutions. *J. Phys. Chem. B* **2006**, *110*, 313−318.
(47) Ramanan, H.; Kokkoli, E.; Tsapatsis, M. On the TEM and AFM evidence of zeosil nanoslabs present during the synthesis of silicalite-1. *Angew. Chem., Int. Ed.* **2004**, *43*, 4558−4561.
(48) Feng, S.; Bein, T. Growth of oriented molecular sieve crystals on organophosphonate films. *Nature* **1994**, *368*, 834−836.
(49) Lai, Z. P.; Bonilla, G.; Diaz, I.; Nery, J. G.; Sujaoti, K.; Amat, M. A.; Kokkoli, E.; Terasaki, O.; Thompson, R. W.; Tsapatsis, M.; Vlachos, D. G. Microstructural optimization of a zeolite membrane for organic vapor separation. *Science* **2003**, *300*, 456−460.
(50) Pradhan, A. R.; Macnaughtan, M. A.; Raftery, D. Zeolite-coated optical microfibers for intrazeolite photocatalysis studied by in situ solid-state NMR. *J. Am. Chem. Soc.* **2000**, *122*, 404−405.
(51) Nguyen, T.-Q.; Wu, J.; Doan, V.; Schwartz, B. J.; Tolbert, S. H. Control of energy transfer in oriented conjugated polymer-mesoporous silica composites. *Science* **2000**, *288*, 652−656.
(52) Calzaferri, G.; Bossart, O.; Bruhwiler, D.; Huber, S.; Leiggener, C.; Van Veen, M. K.; Ruiz, A. Z. Light-harvesting host-guest antenna materials for quantum solar energy conversion devices. *C. R. Chim.* **2006**, *9*, 214−225.
(53) Kim, H. S.; Lee, S. M.; Ha, K.; Jung, C.; Lee, Y.-J.; Chun, Y. S.; Kim, D.; Rhee, B. K.; Yoon, K. B. Aligned inclusion of hemicyanine dyes into silica zeolite films for second harmonic generation. *J. Am. Chem. Soc.* **2004**, *126*, 673−682.
(54) Bein, T. Zeolitic host-guest interactions and building blocks for the self-assembly of complex materials. *MRS Bull.* **2005**, *30*, 713−720.
(55) Schüth, F.; Schmidt, W. Microporous and Mesoporous Materials. *Adv. Mater.* **2002**, *14*, 629−638.

AR000119C